

# Studies on the controlled morphology and wettability of polystyrene surfaces by electrospinning or electrospraying

Jianfen Zheng, Aihua He\*, Junxing Li, Jian Xu, Charles C. Han\*

*Beijing National Laboratory for Molecular Sciences, Joint Laboratory of Polymer Science and Materials, State Key Laboratory of Polymer Physics and Chemistry, Institute of Chemistry, Chinese Academy of Sciences, Beijing 100080, PR China*

Received 8 June 2006; received in revised form 8 August 2006; accepted 9 August 2006

Available online 30 August 2006

## Abstract

Polystyrene (PS) surfaces with various morphologies have been produced by electrospinning or electrospraying, such as beads with different sizes and shapes, bead-on-string structures with different aspect ratios of the beads and fibers with different diameters and shapes. Both the solution properties and the electrospinning conditions affected the PS surface morphology obtained. The results of water contact angle (CA) measurement indicated that the surface morphology could affect the wettability distinctively. It was found that CA values of PS surfaces comprised merely fibers were in the range of  $140^{\circ}$ – $150^{\circ}$ . The CA values of PS surfaces comprised bead-on-string structures were usually about  $150^{\circ}$ . However, the CA values of PS surfaces consisted of particles could reach up to  $160^{\circ}$ , which shows a superhydrophobic property. A bilayer fibers-on-beads surface was verified to be stable and superhydrophobic.

© 2006 Elsevier Ltd. All rights reserved.

**Keywords:** Polystyrene; Electrospinning; Wettability

## 1. Introduction

Wettability is one of the most important properties of solid surfaces for both fundamental research and practical applications. Functional surfaces with special wettability play an important role in our daily life, as well as in industry and agriculture applications. For example, the superhydrophobic surfaces may have self-cleaning properties with potential applications in the anti-contamination field [1].

Although both surface energy and surface roughness are the dominant factors for wettability of materials, surface roughness is the key factor once the components of materials have been selected. A material with the lowest surface energy ( $6.7 \text{ mJ/m}^2$  for a surface with regularly aligned closest-hexagonal-packed- $\text{CF}_3$  groups) gives a CA only around  $120^{\circ}$  [2,3], while a hydrophilic material can produce surfaces with water

contact angle larger than  $150^{\circ}$  after surface decoration [4,5]. Cassie and Baxter proposed Eq. (1) to describe the relationship between the CA of a water droplet on a smooth surface ( $\theta$ ) and the CA of a water droplet on a rough surface ( $\theta_r$ ) composed of solid and air.

$$\cos \theta_r = f_1 \cos \theta - f_2 \quad (1)$$

in which  $f_1$  and  $f_2$  are the fractions of solid/water interface and air/water interface, respectively, and  $f_1 + f_2 = 1$ .

There are various methods to produce rough surfaces [1], such as laser ablation and photolithography-based microfabrication, solidification of melted alkylketene dimer, microwave plasma-enhanced CVD of trimethoxymethoxysilane, phase separation, domain-selective oxygen plasma treatment, sol–gel method, electrospinning or electrospraying and so on. It is believed that electrospinning or electrospraying is a simple and effective way to fabricate various polymer surfaces, such as beads' structure, bead-on-string structure, ribbon-like and rounded fibers in the range of micro- to nanometer [6–8]. Generally speaking, fibers could be produced during electrospinning

\* Corresponding authors. Tel.: +86 10 82618089; fax: +86 10 62521519 (C.C.H.).

E-mail address: [c.c.han@iccas.ac.cn](mailto:c.c.han@iccas.ac.cn) (C.C. Han).

process, and beads could be produced during electrospinning process.

Spinning solution parameters (solution viscosity, surface tension, molecular weight of the polymer, etc.), and electrospinning parameters (applied voltage, solution feeding rate, tip-to-collector distance, etc.) are the main factors that influence the electrospinning process. By changing the electrospinning conditions, polymer surfaces with various fiber and bead morphologies can be obtained [9–11]. In Shenoy's work [12], polymer solution rheology arguments have been extrapolated to formulate a semi-empirical analysis to explain the transition from electrospinning to electrospinning in good solvent, non-specific polymer–polymer interaction limit. Supaphol's group studied the effects of solvents on the electrospinning process of PS solution and obtained PS surface morphologies [13,14]. Reneker's group [15] observed branched fibers, flat ribbons, ribbons with other shapes, and fibers that were split longitudinally from larger fibers. Fluid mechanical effects, electrical charge carried with the jet, and evaporation of the solvent were believed to contribute to the formation of the fibers. Micro- and nano-structured surface structures which were referred to as a “porous” morphology was observed by Rabolt's group on electrospun PS, PMMA and PC fibers [16,17].

Jiang et al. [18] reported a lotus-leaf-like microsphere/nanofiber composite film of PS by electrohydrodynamics method, which afforded superhydrophobicity ( $CA = 160.4^\circ$ ). Block copolymer poly(styrene-*b*-dimethylsiloxane) fibers with diameters in the range 150–400 nm were produced by electrospinning, and were found to exhibit superhydrophobicity ( $CA = 163^\circ$ ). The superhydrophobicity is attributed to the combined effects of surface enrichment in siloxane as revealed by X-ray photoelectron spectroscopy and surface roughness of the electrospun mat itself [19].

PS, which is one of the most used plastics was used in our study. PS belongs to amorphous polymer and the CA value of its spin-coated membrane is about  $97^\circ$ . The polymer surfaces with different morphologies produced by electrospinning or electrospinning are too complicated to calculate theoretically the wettability of the obtained surfaces. Therefore, the goal of this research is to produce PS surfaces with various morphologies by controlling electrospinning conditions, and then to study the relationship between the surface morphology and its wettability. To the best of our knowledge, a systematic study on the wettabilities of electrospun or electrospayed polymer surfaces with various morphologies has not been reported before.

## 2. Experimental

### 2.1. Materials

The amorphous PS (666D) with average weight molecular weight of 347,000 (g/mol) was purchased from Beijing Yanshan Chem. Co. Ltd. (Beijing, China). The PS with weight molecular weight of 7400 was kindly supplied by group of Jian Xu, Institute of Chemistry, Chinese Academy of Science. PS used in the experiment was with molecular weight of 347,000 if there is no other specification. Hexadecyltrimethyl

ammonium bromide (RN) was purchased from Beijing Chem. Co. (Beijing, China). The solvents used in this work were *N,N*-dimethyl formamide (DMF, Beijing Xingjin Chem. Co.), tetrahydrofuran (THF, Beijing Chem. Co.) and mixture of DMF and THF. All the materials were used without further purification.

### 2.2. Characterization of PS and PS solutions

PS solutions were prepared at room temperature by dissolving a measured amount of PS pellets in solvent and stirring gently to form transparent solutions. Viscosities of these PS solutions were characterized by using a digital Couette viscometer (NDJ-8S, China). Surface tensions of these solutions were measured through surface tension meter (Dataphysics, DCAT 21, Germany). The conductivity was measured by conductivity meter (DDS-307, Rex Shanghai, China). All the solution properties were characterized at temperature corresponding to the electrospinning.

### 2.3. Electrospinning setup

DC high-voltage generator (The Beijing Machinery & Electricity Institute, China) was applied to produce voltages ranging from 0 to 50 kV. The electrospinning solutions were placed into a 5 mL syringe with a capillary tip having an inner diameter of 0.3 mm. A syringe pump was used to feed polymer solution into the needle tip. A sheet of aluminum foil, connected to the ground, was placed under the syringe as collector. The temperature ( $T$ ) was fixed at  $46^\circ\text{C}$ , the voltage ( $V$ ) at 15 kV, the feeding rate ( $v$ ) at  $45\ \mu\text{L}/\text{min}$ , and the tip-to-collector distance ( $d$ ) at 15 cm if there is no other specification. The temperature of electrospinning solutions, syringe and environment varied from room temperature to  $70^\circ\text{C}$ . Humidity of the electrospinning environment was also considered, and controlled at around 40%.

### 2.4. Characterization of electrospun or electrospayed PS surfaces

The morphologies of electrospun or electrospayed PS surfaces were observed with scanning electron microscope (SEM, Hitachi, S-4300, Japan). Each sample was sputter-coated with gold for analysis. The wettability of PS surface was characterized on a homemade instrument at ambient circumstance. CA was measured using a sessile drop method. CA values of the right side and the left side of the water droplet are both measured, and an average value is used. All the CA data were an average of five measurements on different locations of the surface. A water drop of  $5\ \mu\text{L}$  was used.

## 3. Results and discussion

Usually three typical morphologies such as bead structure, bead-on-string structure and fiber structure can be obtained by adjusting electrospinning conditions, for example, solvent, polymer molecular weight, polymer concentration, temperature, applied voltage, etc.

DMF, THF and mixed solvent of DMF and THF with different volume ratios were used in this study. The difference between these solvents in boiling point, solubility parameter, dielectric constant, density, etc. may all affect the morphology of the obtained surface. Physical properties such as viscosity, surface tension and conductivity of the PS solutions in different solvents with concentration of 10% (w/v) were measured and are listed in Table 1. Two series of PS solutions with increasing concentrations from 5% to 30% (w/v) in DMF and THF were also prepared, respectively. The viscosity, surface tension and the conductivity of these PS solutions were measured and are listed in Table 2. In our study, one kind of ammonium salt compound (RN) was used to increase the conductivity of PS solutions. Two kinds of PS with different molecular weights were used to study the effect of molecular weight of PS on the surface morphology. In addition, processing parameters such as feeding rate, tip-to-collector distance, etc. have also been studied to fabricate varied morphological surfaces. As a result, beads with different sizes and shapes, bead-on-string structure with different aspect ratios of the beads and fibers with different diameters and shapes were obtained.

### 3.1. PS beads

Generally, beads are produced when the spinning solution is fairly diluted due to high surface tension of the solution and the insufficient viscosity and electrical conductivity of the solution. Therefore, PS solutions with low concentrations and low molecular weight were used in the electrospinning process.

In our study, four kinds of PS particles were prepared by electrospinning, as shown in Fig. 1. When the concentration of PS in THF was 5% (w/v), beads with a collapsed surface were produced, and the average bead size was about 10  $\mu\text{m}$ , as shown in Fig. 1(a). Half hollow spheres [16] with average diameter around 20  $\mu\text{m}$  occurred when the concentration of PS increased to 10%, as shown in Fig. 1(d). Nanopores were observed on the above two kinds of particles at high magnification (Fig. 1(c,f)). The pore size of particles in Fig. 1(c) was ranging from 50 to 200 nm. However, it was found that the pore size in Fig. 1(f) was centered around 100 nm. The above two kinds of PS particles were electrospun at 26 °C. Particles in Fig. 1(g) are electrospun from PS/DMF solution with concentration of 5% (w/v). Beads with size ranging from 0.5 to 3  $\mu\text{m}$  were produced. The surface of the beads

Table 1  
Properties of PS solutions in DMF–THF mixed solvents

Properties	DMF/THF (volume ratio)				
	100/0 <sup>a</sup>	75/25 <sup>a</sup>	50/50 <sup>a</sup>	25/75 <sup>a</sup>	0/100 <sup>b</sup>
Viscosity (Pa s)	0.018	0.015	0.015	0.016	0.021
Surface tension (mN/m)	34.339	31.489	29.198	26.969	24.735
Conductivity ( $\mu\text{S}/\text{cm}$ )	2.40	1.80	1.34	0.54	$\sim 0$

All solutions were prepared with concentration of 10% (w/v).

<sup>a</sup> Measured at 46 °C, corresponding to electrospinning condition.

<sup>b</sup> Measured at 26 °C, corresponding to electrospinning condition.

Table 2  
Properties of PS solutions in DMF and THF with different concentrations

Properties	Concentration (w/v%)			
	5	10	20	30
Viscosity (Pa s)				
DMF <sup>a</sup>	0.006	0.018	0.106	0.354
THF <sup>b</sup>	0.007	0.029	0.133	0.495
Surface tension (mN/m)				
DMF <sup>a</sup>	33.894	34.339	34.773	34.882
THF <sup>b</sup>	27.034	26.896	27.932	25.877
Conductivity ( $\mu\text{S}/\text{cm}$ )				
DMF <sup>a</sup>	6.08	2.40	1.70	1.24
THF <sup>b</sup>	$\sim 0$	$\sim 0$	$\sim 0$	$\sim 0$

The viscosity of PS/THF solution with concentration of 30% was measured with rotor 2# at 30 r/min, while others at 60 r/min.

<sup>a</sup> Measured at 46 °C, corresponding to electrospinning condition.

<sup>b</sup> Measured at 26 °C, corresponding to electrospinning condition.

was really rough with many nano-sized papillae. A few fibers with diameter around 45 nm could also be observed as shown in Fig. 1(g). Irregularly shaped beads without nano-structure on the surface were produced from 20% (w/v) PS/DMF solution with a lower molecular weight PS (74,000), as shown in Fig. 1(j).

The CA of the above four kinds of surfaces was  $157.6 \pm 1.6^\circ$ ,  $153.3 \pm 0.9^\circ$ ,  $159.5 \pm 3.0^\circ$  and  $152.9 \pm 1.7^\circ$ , respectively. It was found that the PS surfaces composed of beads usually have CA values ranging from  $153^\circ$  to  $160^\circ$ . Generally, the CA value of a casting PS film is only about  $97^\circ$ . The change in surface morphology of PS leads to the big increase in CA value, which means that the wettability of the PS surface could be changed distinctly. More air can be trapped as the roughness of PS surface increases. According to Cassie equation, an increase in the fraction of air surface brings an increase in CA of the surface, and thus brings an increase in hydrophobicity of the surface.

### 3.2. Bead-on-string structure

Bead-on-string structure is the morphology between bead structure and fiber structure, and usually occurred when the concentration of dilute polymer solution increased. The bead size and aspect ratio of the beads on string could be adjusted by using different solvents.

Bead-on-string structures with different size and aspect ratio of beads were obtained, as shown in Fig. 2. DMF, mixed solvent of DMF–THF with volume ratio of 75/25, 50/50, 25/75 and THF were used in this part. PS surfaces in Fig. 2(a,c,e,g) are obtained from 10% (w/v) PS/DMF–THF solution with DMF/THF volume ratio of 100/0, 75/25, 50/50 and 25/75, respectively. The morphology parameters of the bead-on-string structure are listed in Table 3. It can be seen from Table 3 that fiber diameter and the aspect ratio of beads increased with the decrease of DMF/THF ratio, and also the content of fibers increased. When the volume ratio of DMF/THF was 100/0, the fiber diameter was in the range of 50–200 nm and the average bead aspect ratio was 1.7. When DMF/THF volume

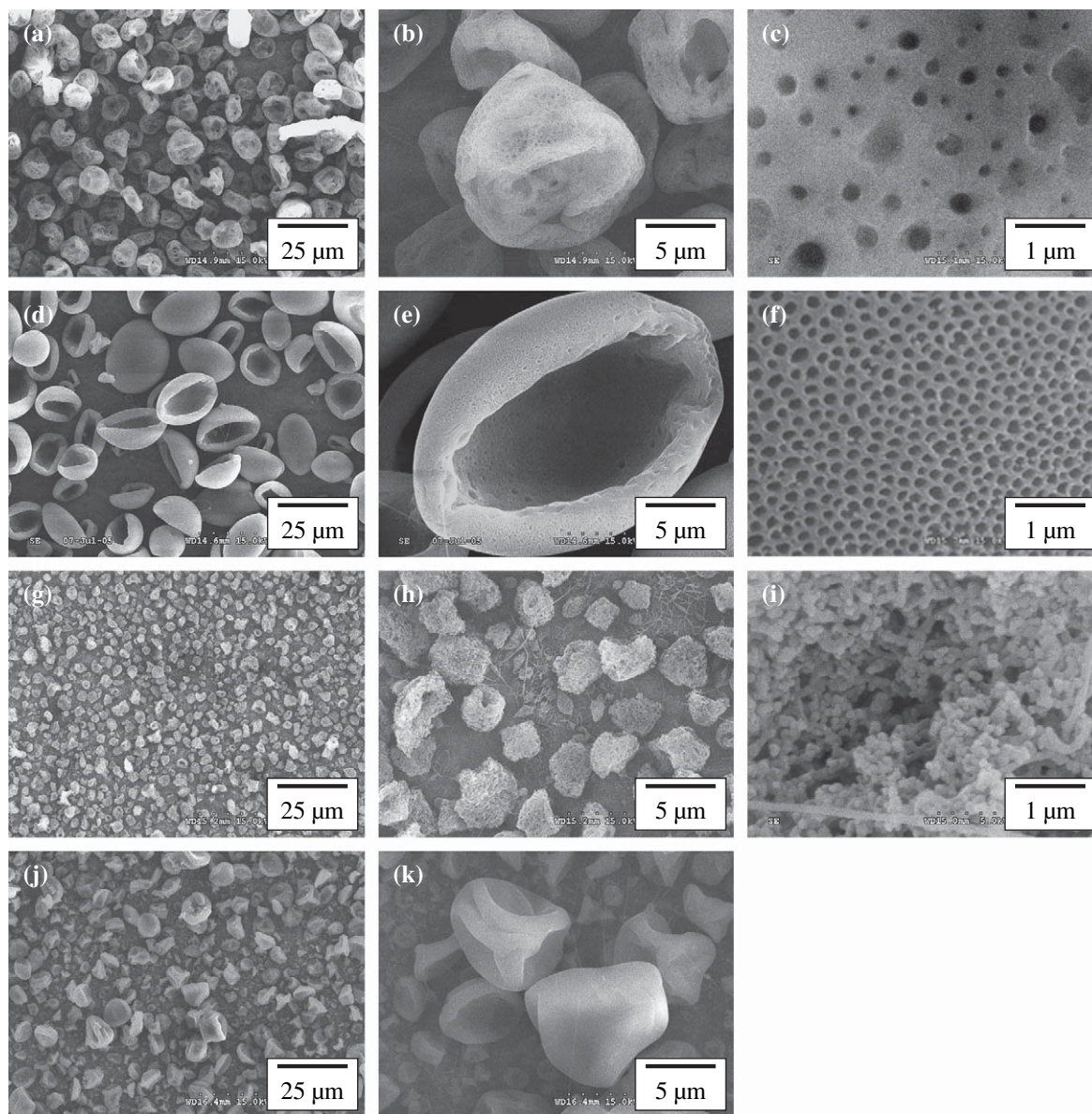


Fig. 1. SEM images of bead morphologies obtained from: (a–c) 5% PS/THF; (d–f) 10% PS/THF; (g–i) 5% PS/DMF solution with PS molecular weight of 347,000; (j,k) 20% PS/DMF solution with PS molecular weight of 74,000.  $V = 15$  kV;  $v = 45$   $\mu$ L/min;  $d = 15$  cm; (a–f)  $T = 26$   $^{\circ}$ C, (g–k)  $T = 46$   $^{\circ}$ C. (a–c)  $CA = 157.6 \pm 1.6^{\circ}$ , (d–f)  $CA = 153.3 \pm 0.9^{\circ}$ , (g–i)  $CA = 159.5 \pm 3.0^{\circ}$ , (j,k)  $CA = 152.9 \pm 1.7^{\circ}$ .

ratio decreased to 25/75, the fiber diameter increased to the range of 300–600 nm and the average bead aspect ratio increased to 5.0. It can be seen from Fig. 2(i) that the bead surface collapsed in a complicated way and pore size on the bead surface was around 100 nm when 20% (w/v) PS/THF solution was electrospun at 26  $^{\circ}$ C. It was also found that the size and depth of pores decreased with the increase in ambient temperature, keeping humidity at 40%, as shown in Fig. 3. The bead size in Fig. 2(i) was ranged from 10 to 30  $\mu$ m and the fiber diameter varied from 1 to 5  $\mu$ m.

The CA of the above five kinds of surfaces in Fig. 2 was  $151.2^{\circ} \pm 1.9^{\circ}$ ,  $151.3 \pm 1.7^{\circ}$ ,  $151.2 \pm 1.6^{\circ}$ ,  $146.3 \pm 1.9^{\circ}$  and  $150.9 \pm 0.7^{\circ}$ , respectively. It was found that the bead-on-string structures usually have CA values ranging from  $146^{\circ}$  to  $151^{\circ}$  and most of the bead-on-string structures have a CA around

$150^{\circ}$ . It is obvious that the low CA value of  $146^{\circ}$  for the morphology shown in Fig. 2(g) can be attributed to its high fiber to bead ratio.

### 3.3. Fibers

When the solution concentration increased to a certain degree, beads disappeared and uniform fibers could be obtained. An increase in solution concentration favors the fiber formation because at high polymer concentration, sufficient chain entanglements serve to stabilize the electrospinning jet by inhibiting jet breakup. But when the concentration is too high, the relatively high viscosity will also inhibit the electrospinning process. Besides increasing the solution concentration, adding of ionic salt to the polymer solution is another

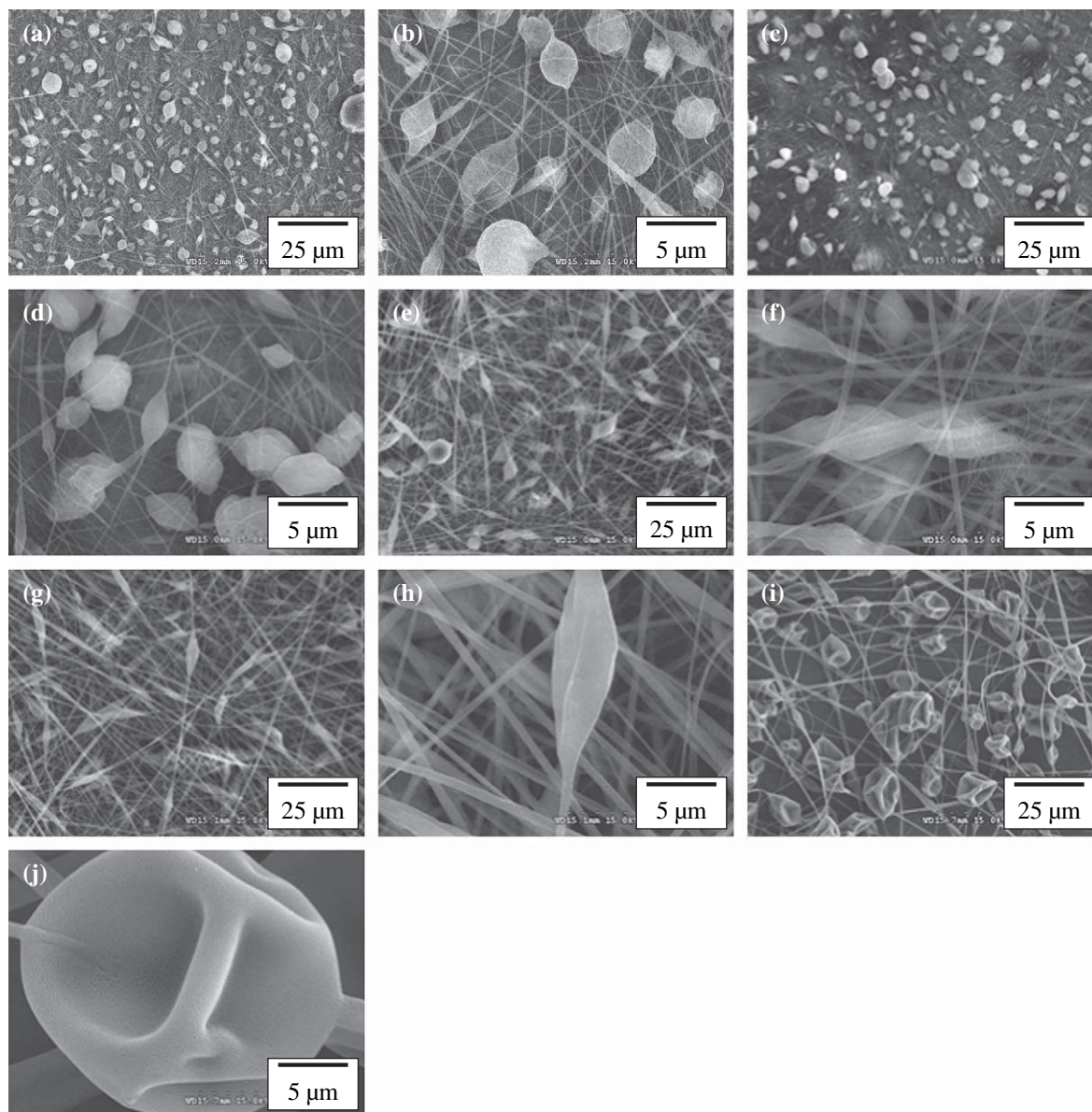


Fig. 2. SEM images of bead-on-string morphologies obtained from: (a,b) 10% PS/DMF; (c,d), (e,f), and (g,h) 10% PS/DMF–THF. (c,d) DMF/THF = 75/25; (e,f) DMF/THF = 50/50 and (g,h) DMF/THF = 25/75; (i,j) 20% PS/THF.  $V = 15$  kV,  $v = 45$   $\mu\text{L}/\text{min}$ ,  $d = 15$  cm, (i,j)  $T = 26$   $^{\circ}\text{C}$ , others  $T = 46$   $^{\circ}\text{C}$ . (a,b)  $\text{CA} = 151.2^{\circ} \pm 1.9^{\circ}$ , (c,d)  $\text{CA} = 151.3^{\circ} \pm 1.7^{\circ}$ , (e,f)  $\text{CA} = 151.2^{\circ} \pm 1.6^{\circ}$ , (g,h)  $\text{CA} = 146.3^{\circ} \pm 1.9^{\circ}$  and (i,j)  $\text{CA} = 150.9^{\circ} \pm 0.7^{\circ}$ .

simple and effective way to inhibit the bead formation in electrospinning process and favor the fiber formation.

Four kinds of PS nonwovens with different fiber diameters were obtained, as shown in Fig. 4. Fibers with average

Table 3  
Morphology parameters of electrospun PS surfaces from DMF–THF mixed solvents and their water contact angles

DMF/THF	Fiber diameter (nm)	Bead size ( $\mu\text{m}$ )	Aspect ratio	CA ( $^{\circ}$ )
100/0	50–200	5/3	1.7	$151.2 \pm 1.9^{\circ}$
75/25	50–200	5/3	1.7	$151.3 \pm 1.7^{\circ}$
50/50	200–500	10/3	3.3	$151.2 \pm 1.6^{\circ}$
25/75	300–600	15/3	5.0	$146.3 \pm 1.9^{\circ}$
0/100	—	20	—	$153.3 \pm 0.9^{\circ}$

Note: bead size (bead length along the fibers/bead length perpendicular to the fiber).

diameter of 55 nm and also a few beads were electrospun from 5% (w/v) PS/DMF solution containing 0.05% (w/v) RN, as shown in Fig. 4(a,b). Uniform fibers with average diameter of 140 nm could be electrospun successfully from 10% (w/v) PS/DMF solution containing 0.1% (w/v) RN, as shown in Fig. 4(c,d). The feeding rate of the above two samples was decreased from 45 to 20  $\mu\text{L}/\text{min}$  to stabilize the electrospinning process, with little change of surface morphology. It was found that the surface morphologies had been totally changed by adding RN when compared to PS/DMF solution with the same concentration without adding RN, as shown in Figs. 1(g) and 2(c). The content of beads was dramatically decreased and finally disappeared with the addition of RN. The conductivity of the PS solution with RN was greatly increased, as shown in Table 4. The increase in

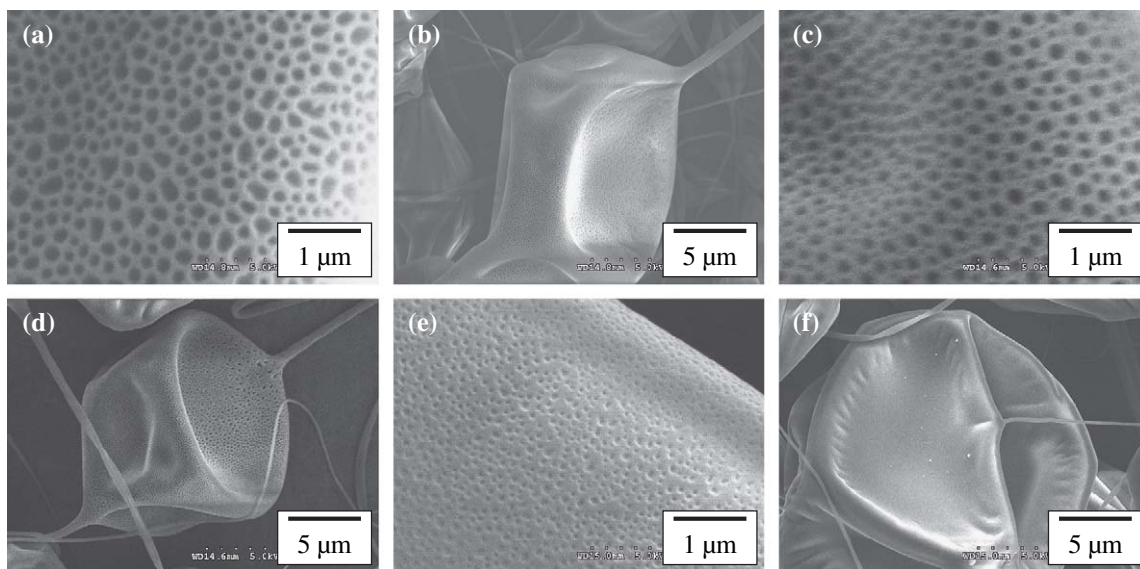


Fig. 3. SEM images of electrospun PS from 20% PS/THF solutions at different ambient temperatures: (a,b) 26 °C, (c,d) 36 °C and (e,f) 46 °C.  $V = 15$  kV,  $v = 45$   $\mu\text{L}/\text{min}$ ,  $d = 15$  cm.

conductivity benefits the fiber formation. When the concentration of PS/DMF solution increased to 30% (w/v), uniform fibers with average diameter of 1.73  $\mu\text{m}$  were produced as shown in Fig. 4(e). However, ribbon-like fibers with size

around 10  $\mu\text{m}$  were produced from 30% PS/THF solution at 26 °C, as shown in Fig. 4(g). Through SEM images of high magnification, nano-structured surface morphology was observed and the pore size was around 200 nm.

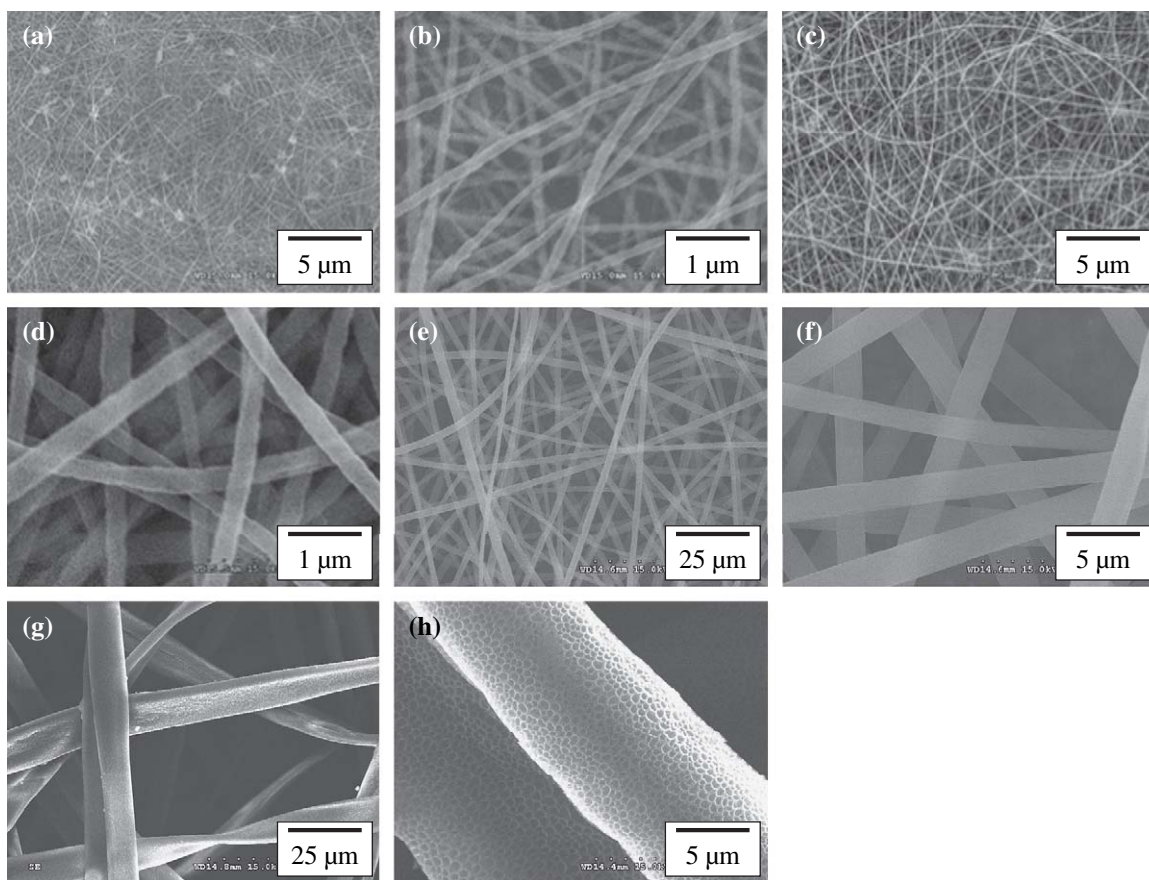


Fig. 4. SEM images of fiber morphologies obtained from: (a,b) 5% PS/DMF solution with  $C_{RN} = 0.05\%$ ; (c,d) 10% PS/DMF solution with  $C_{RN} = 0.10\%$ ; (e,f) 30% PS/DMF solution; and (g,h) 30% PS/THF solution.  $V = 15$  kV,  $d = 15$  cm,  $T = 46$  °C, (a–d)  $v = 20$   $\mu\text{L}/\text{min}$ , (e–h)  $v = 45$   $\mu\text{L}/\text{min}$ . (a,b)  $CA = 142.7 \pm 1.3^\circ$ ; (c,d)  $CA = 148.5 \pm 2.4^\circ$ ; (e,f)  $CA = 152.9 \pm 1.7^\circ$ ; (g,h)  $CA = 146.6 \pm 1.8^\circ$ .

Table 4  
Conductivity ( $\mu\text{S}/\text{cm}$ ) of PS/DMF solutions with and without RN

$C_{\text{RN}}$ (w/v%)	$C_{\text{PS}}$ (w/v%)	
	5	10
0	6.08	2.40
0.05	—	78.8
0.10	155.8	—

Note: all measured at 46 °C, corresponding to electrospinning condition.

The CA of the above four kinds of surfaces was  $142.7 \pm 1.3^\circ$ ,  $148.5 \pm 2.4^\circ$ ,  $152.9 \pm 1.7^\circ$  and  $146.6 \pm 1.8^\circ$ , respectively. It can be seen that CA values of most of the nonwovens were ranging from  $143^\circ$  to  $153^\circ$ . The relatively high CA ( $152.9^\circ$ ) of the PS surface may be caused by the right fiber diameter and pore size which could trap more air in the inter-space than other fiber structures.

### 3.4. Further discussion

From all the samples presented above, we can see that beads and fibers produced from PS/THF solution are larger in size compared to that produced from PS/DMF solution. That is probably due to the poor conductivity of THF and the PS/THF solutions, as listed in Table 2. The conductivities of PS/THF solutions with different concentrations were close to zero. During electrospinning process, the electric force was the driving force and the enhanced charge density could benefit the whipping instability, which leads to further thinning of the jet when it leaves away from the nozzle. This process may be inhibited for PS/THF solution due to the poor conductivity of THF, thus leads to larger size of electrospayed or electrospun PS beads or fibers. For all the samples produced from PS/THF solutions, nanopores were observed on the beads or fibers. It had been reported that the high humidity of

ambient environment and high volatility of the solvent often lead to the formation of pores on electrospun fibers. In our study, we further investigated that the size and depth of pores decreased with the increase in ambient temperature. Vapor-induced phase separation might be the mechanism for the pore formation. During vapor-induced phase separation the polymer solution undergoes phase separation by penetration of nonsolvent from the vapor phase. When the temperature increases, THF vaporizes at much higher rate therefore the process of phase separation is unable to take place sufficiently before THF is completely vaporized. Another mechanism may be considered in the formation of pores is the breath figures formation. During electrospinning process the solvent evaporates so rapidly that the temperature of the fiber surface decreases significantly. As the surface cools down moisture in the air may be condensed and grew in the form of droplets. An imprint will be left on the surface of the fibers or beads during the drying process. As the environment temperature increases, condensation of water droplets becomes more difficult and smaller water droplets may be formed if they can form at all. Thus the imprinted pores will have smaller size and depth. Vapor-induced phase separation and breath figure are the two possible mechanisms for the pore formation in electrospinning process. Further study is needed to verify which one is the really dominant process and how does the process take place.

For PS solution in DMF and THF mixed solvent with concentration of 10%, the solution viscosity does not change obviously with the change of DMF/THF volume ratio. Both surface tension and conductivity of the solution decrease with the increasing content of THF, as listed in Table 1. Therefore, with the help of volume ratio of DMF/THF, both surface tension and conductivity of the PS solutions could be adjusted which might lead to changed electrospinning process. The

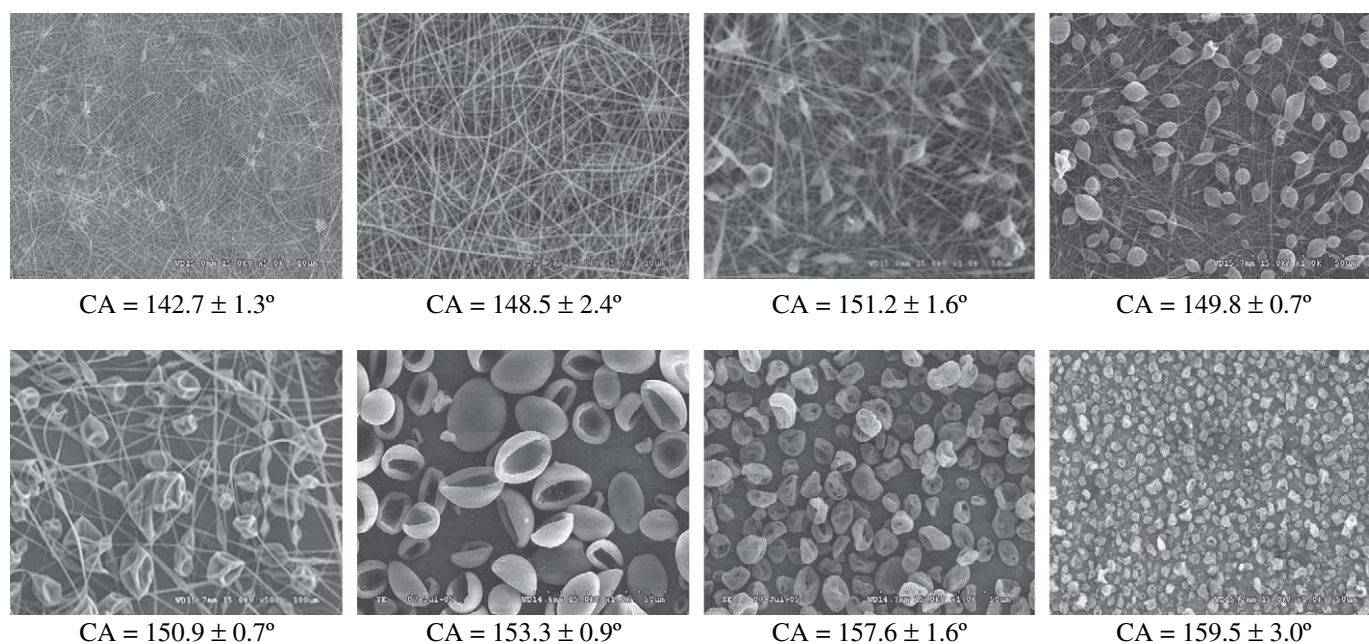


Fig. 5. Various surface morphologies produced by electrospinning or electrospaying and corresponding water contact angles.

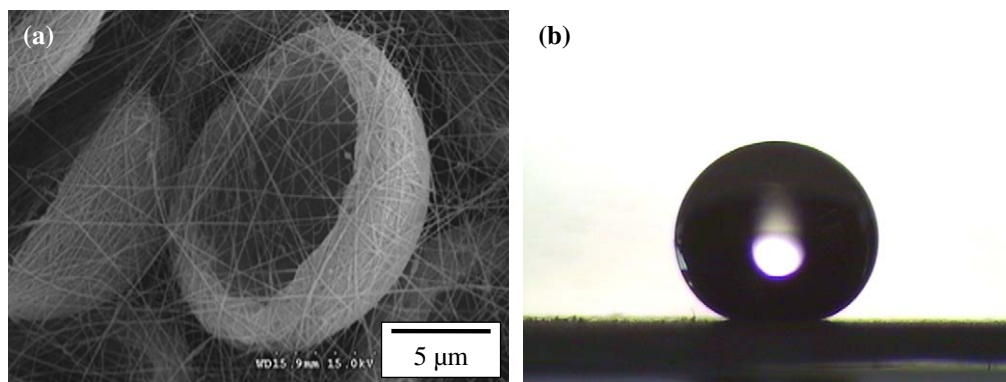


Fig. 6. (a) SEM image of bilayer structured PS surfaces prepared from 10% PS/THF solution and 5% PS/DMF solution with RN in it.  $C_{RN} = 0.10\%$  and (b) a water droplet on the surface.  $CA = 158.1 \pm 2.4^\circ$ .

fiber diameter and the size of beads in the PS surfaces obtained with different DMF/THF volume ratios are listed in Table 3. For the two series of PS solution in DMF and THF, the viscosity of the solutions increases obviously with the increase in concentration, while surface tension of these solutions does not change much. The conductivity of PS solution in DMF decreases with the increase of PS concentration, while all PS solution in THF tends to zero. Therefore, the increase in solution concentration leads to a morphology change from beads to fibers as well as an increase in fiber diameter.

Fig. 5 shows the typical morphologies obtained in our experiments and their water contact angles. It can be seen from Fig. 5 that surfaces containing merely fibers usually have relatively low CA in the range of  $140^\circ$ – $150^\circ$ , bead-on-string structure usually gives CA around  $150^\circ$ , while surfaces composed of beads are the most hydrophobic, and their CA is usually larger than  $150^\circ$ . However, during the measurements of CA, some clusters of PS particles often floated on the surfaces of water droplets. In order to solve this problem, a super-thin layer of PS nanofibers was electrospun on the PS particles, in which the average diameter of upper-layer fibers was about 50 nm, as shown in Fig. 6. This surface has CA of  $158.1 \pm 2.4^\circ$ . In this way, a stable PS surface with super-hydrophobicity could be obtained.

#### 4. Conclusion

Various surface morphologies have been produced by electrospinning or electro spraying: beads with different sizes and shapes, bead-on-string structure with different aspect ratios of the beads and fibers with different diameters and shapes. Physical properties of the PS solutions such as viscosity, surface tension and conductivity greatly influence the electrospun or electro sprayed PS morphology. Low surface tension and high viscosity benefit the fiber formation, and low conductivity brings about an increase in fiber and bead size. It was also found that high humidity of ambient circumstance and high volatility of the solvent often lead to the formation of pores on the surface of PS beads or fibers.

By the measurement of water contact angle, we can see that different morphologies correspond to different water contact angles, which indicate different wettability of the surface.

We can conclude that the wettability of a solid surface is greatly influenced by its surface morphology: a spin-coated PS membrane has a water contact angle of  $97^\circ$ , while electrospun PS membranes have water contact angles around  $150^\circ$ . The most hydrophobic membrane has a water CA of  $159.5^\circ$ . Moreover, a stable bilayer fibers-on-beads surface with CA of  $158.1 \pm 2.4^\circ$  has been produced.

#### Acknowledgements

This work was financially supported by the National Nature Science Foundation of China (Funds Nos. 50503023 and 50373048), the National “973” Project (G2003 CB615605), the MSC Creative Project of CAS (CMS-CX200503).

#### References

- [1] Sun TL, Feng L, Gao XF, Jiang L. *Acc Chem Res* 2005;38:644–52.
- [2] Nishino T, Meguro M, Nakamae K, Matsushita M, Ueda Y. *Langmuir* 1999;15:4321–3.
- [3] Miwa M, Nakajima A, Fujishima A, Hashimoto K, Watanabe T. *Langmuir* 2000;16:5754–60.
- [4] Guo CW, Feng L, Zhai J, Wang GJ, Song YL, Jiang L, et al. *Chem Phys Chem* 2004;5:750–3.
- [5] Sun TL, Wang GJ, Feng L, Liu BQ, Ma YM, Jiang L, et al. *Angew Chem Int Ed* 2004;43:357–60.
- [6] Li Dan, Xia Younan. *Adv Mater* July 19, 2004;16(14).
- [7] Huang ZM, Zhang YZ, Kotaki M, Ramakrishna S. *Compos Sci Technol* 2003;63:2223–53.
- [8] Acatay K, Simsek E, Yang C, Menciloglu YZ. *Angew Chem Int Ed* 2004;43:5210–3.
- [9] Liu J, Kumar S. *Polymer* 2005;46:3211–4.
- [10] Fong H, Chun I, Reneker DH. *Polymer* 1999;40:4585–92.
- [11] Lee KH, Kim HY, Bang FJ, Jung YH, Lee SG. *Polymer* 2003;44:4029–34.
- [12] Shenoy SL, Bates WD, Frisch HL, Wnek GE. *Polymer* 2005;46:3372–84.
- [13] Wannatong L, Sirivat A, Supaphol P. *Polym Int* 2004;53:1851–9.
- [14] Jarusuwannapoom T, Hongrojjanawiwat W, Jirjaicham S, Wannatong L, Nithitanakul M, Pattamaprom C, et al. *Eur Polym J* 2005;41:409–21.
- [15] Koombhongse S, Liu W, Reneker DH. *J Polym Sci Part B Polym Phys* 2001;39:2598–606.
- [16] Megelski S, Stephens JS, Chase DB, Rabolt JF. *Macromolecules* 2002;35:8456–66.
- [17] Casper CL, Stephens JS, Tassi NG, Chase DB, Rabolt JF. *Macromolecules* 2004;37:573–8.
- [18] Jiang L, Zhao Y, Zhai J. *Angew Chem Int Ed* 2004;43:4338–41.
- [19] Ma ML, Hill RM, Lowery JL, Fridrikh SV, Rutledge GC. *Langmuir* 2005;21:5549–54.